



Contents lists available at ScienceDirect

Materials Letters

journal homepage: www.elsevier.com/locate/matlet

Physical and electromechanical properties of barium zirconium titanate synthesized at low-sintering temperature

Nawal Binhayeenyi^a, Pisan Sukvisut^a, Chanchana Thanachayanont^b, Supasarote Muensit^{a,c,*}

^a Department of Physics, Prince of Songkla University (PSU), Songkhla, Thailand

^b National Metal and Materials Technology Center, 114 Thailand Science Park, Pathumthani, Thailand

^c NANOTEC CENTER of Excellence at Prince of Songkla University, Hat yai, Songkhla 90112, Thailand

ARTICLE INFO

Article history:

Received 9 September 2009

Accepted 29 October 2009

Available online xxx

Keywords:

Sol–gel

Sintering aid

Piezoelectricity

Barium zirconium titanate

Raman spectroscopy

ABSTRACT

Barium zirconium titanate or $(\text{Ba}(\text{Zr}_x\text{Ti}_{1-x})\text{O}_3, \text{BZT})$ was prepared using homogeneous BZT powders derived from a sol–gel process. With a sintering aid, the firing temperature for the BZT ceramics was lower by about 30%, meanwhile, the electromechanical properties of the material were not degraded. Crystallographic phases of the BZT system were identified by the XRD data and Raman spectra and we found that the orthorhombic–perovskite BZT ceramic with $x=0.05$ has the best dielectric and piezoelectric properties.

© 2009 Published by Elsevier B.V.

1. Introduction

Due to environmental concerns, lead-free ceramics such as KNN, NBT, and BT [1] have been growing interest in applications such as actuators and sensors. Among them, barium zirconate titanate ($\text{Ba}(\text{Zr}_x\text{Ti}_{1-x})\text{O}_3, \text{BZT}$) has become most attractive. Because it is derived from two perovskite lattices, i.e., barium titanate (BaTiO_3) and barium zirconate (BaZrO_3) and there have been reported that the zirconium substitutions into the titanium lattices enhance the dielectric and piezoelectric properties [2,3]. The BZT-based materials, therefore, have high potential for use as active elements in microfabricated devices [4–6]. However, in promoting the product development, the importance in using the materials of fine particle sizes with homogeneous distribution must be taken into account. In addition, the materials for using as electrodes and interconnects should be relatively inexpensive and should have lower energy consumption. Under common preparation conditions, ceramic materials generally have high sintering temperatures. We thus aim to prepare the homogeneous BZT ceramics with some additives to permit the densification of the BZT at low temperature. The BZT powders obtained from the process are then attractive as starting materials for nowadays technologies in which conventional conductive materials such as silver or gold are used. According to the reports of using Li_2O and LiF as sintering additives for BT and BST systems [5,6], the Li_2O sintering aid was selected and its effect on the physical and electromechanical

properties of the BZT with various zirconium contents in this work was evaluated.

2. Experimental procedures

In the sol–gel route [7], barium acetate [$\text{Ba}(\text{CH}_3\text{COO})_2$, Ajax Finechem], zirconium (IV) propoxide [$\text{C}_{12}\text{H}_{28}\text{O}_4\text{Zr}$, Aldrich, 70 wt.% solution in 1-propanol], and titanium (IV) isopropoxide [$\text{C}_{12}\text{H}_{28}\text{O}_4\text{Ti}$, Aldrich, 97% purity] were the starting materials. Acetic acid (Merck, 100% purity) and 2-methoxyethanol ($\text{CH}_3\text{OCH}_2\text{CH}_2\text{OH}$, Ajax Finechem) were the solvent. In the BZT powder preparation the gels were kept in an oven until dried. Some of the dried gel were calcined at 1100 °C for 2 h. The calcined powder was pressed into a pellet of a diameter of 13 mm and sintered at 1250 °C. Similarly, the rest of the dried gel was added 1.5 wt.% of lithium oxide powders (Li_2O , Aldrich, 97% purity) and homogeneously mixed before being calcined at 700 °C, 10 h. The BZT disks obtained from these powders were sintered at 900 °C, 4 h. The ceramics' morphology was observed by using a scanning electron microscopy (SEM) and were subsequently crushed to determine an average particle size by using a transmission electron microscopy (TEM). The crystal structure of all the samples was analyzed using an X-ray diffractometer (Philips X'pert X-ray diffraction system) with Ni filtered $\text{CuK}\alpha$ radiation and Raman spectroscopy (NT_MDT; NTEGRA spectra). An optical objective lens with 100× was used for focusing the 633 nm radiation from a coherent He–Ne laser on the samples. For electrical measurements, a silver paste was used as the electrodes. To activate the electromechanical response, the electroded samples were poled at an electric field of 3 kV mm^{-1} for 30 min in silicone oil [8]. A LCR meter, Hewlett

* Corresponding author. Tel.: +6674288727; fax: +6674212817.
E-mail address: supasarote.m@psu.ac.th (S. Muensit).

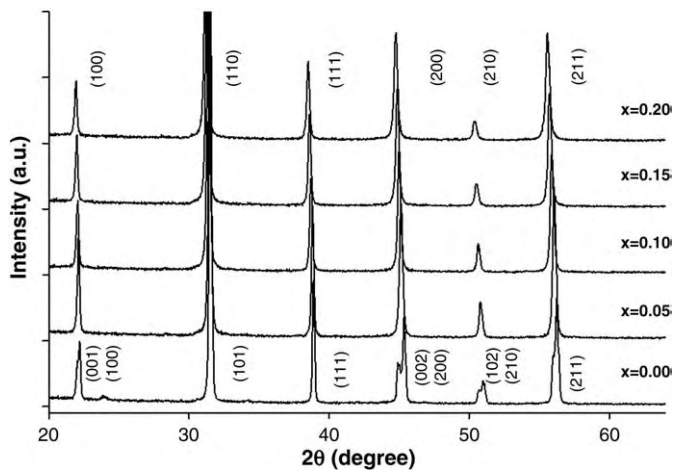


Fig. 1. The XRD patterns of BZT powders calcined at 1100 °C, 2 h.

For the BZT samples with small increment of zirconium content, i.e., $0.00 < x < 0.02$, it was not possible to identify the crystalline phase due to the close proximity of the diffraction angles. Their phases were further observed from the Raman spectrum at room temperature (Fig. 2). Due to the random grain orientation of the BZT powders the direction of the phonon wave vectors is random from one grain to the others with respect to the crystallographic axes [11,12]. The Raman line of the powders shows a mixing mode. When the titanium ions were replaced by the zirconium ions more than 10 wt.%, the Raman mode of $\sim 125 \text{ cm}^{-1}$ was absent. When the Zr content reached 10 mol%, the frequency mode was at about 130 cm^{-1} . This is because the ionic radius of the Zr^{4+} ions is larger than that of the Ti^{4+} ions, it indicated that the phase transforms from orthorhombic to rhombohedral [11]. The results also show that there have no changes in crystal structures relating to the LiO_2 because there is no shift in the Raman line (Fig. 2 a and b). The absence of the $180 \text{ cm}^{-1} A_1(\text{TO}_1)$ mode in $\text{Ba}(\text{Zr}_{0.20}\text{Ti}_{0.80})\text{O}_3$ was due to the cubic nature of the BZT with $x = 0.20$ [12].

The SEM images of the BZT ceramics with various compositions were shown in Fig. 3 and a summary of the physical properties was in Table 1. Without sintering aid the grain size of BZT ceramic was rather cubic and significantly decreased when the Li_2O was added. However, the ceramic texture was denser with higher density as observed in the $\text{Ba}(\text{Zr}_{0.05}\text{Ti}_{0.95})\text{O}_3$ sample.

The temperature dependence of the dielectric constant was observed in the BZT without and with sintering aid (Fig. 4). The transition temperatures in the samples with $0.0 < x < 0.2$ were above room temperature and became closer as the unit cell changed toward the cubic structure. At room temperature, the dielectric constant and the loss tangent increased with Zr content. The Zr substitutions lead to a small expansion of the unit cell and thus an increase in net polarization. The $\text{Ba}(\text{Zr}_{0.05}\text{Ti}_{0.95})\text{O}_3$ is good thermally stable and its transition temperature slightly higher after doping. The diffusions of Li^+ ions did not significantly affect the transition because of a small amount of Li_2O . As noticed earlier, there was a large reduction in grain

Packard 4263B, was employed to observe the dielectric properties. The piezoelectric strain coefficient for the ceramic sample was determined by the Piezo d_{33} tester (APC Part number: 90-2030) [9]. A resonance method was used to determine the transverse piezoelectric coefficient [10].

3. Results and discussion

The XRD results of $\text{Ba}(\text{Zr}_x\text{Ti}_{1-x})\text{O}_3$ ceramics display the polycrystalline-perovskite phase at room temperature (Fig. 1). The BaCO_3 (International Centre for Diffraction Data; ICDD No.01-071-2394) was observed and disappeared at high calcination temperature. The crystallographic phase of the BaTiO_3 is tetragonal (ICDD No.01-075-0462) and it is cubic for the $\text{Ba}(\text{Zr}_{0.20}\text{Ti}_{0.80})\text{O}_3$ (ICDD No.00-006-0399).

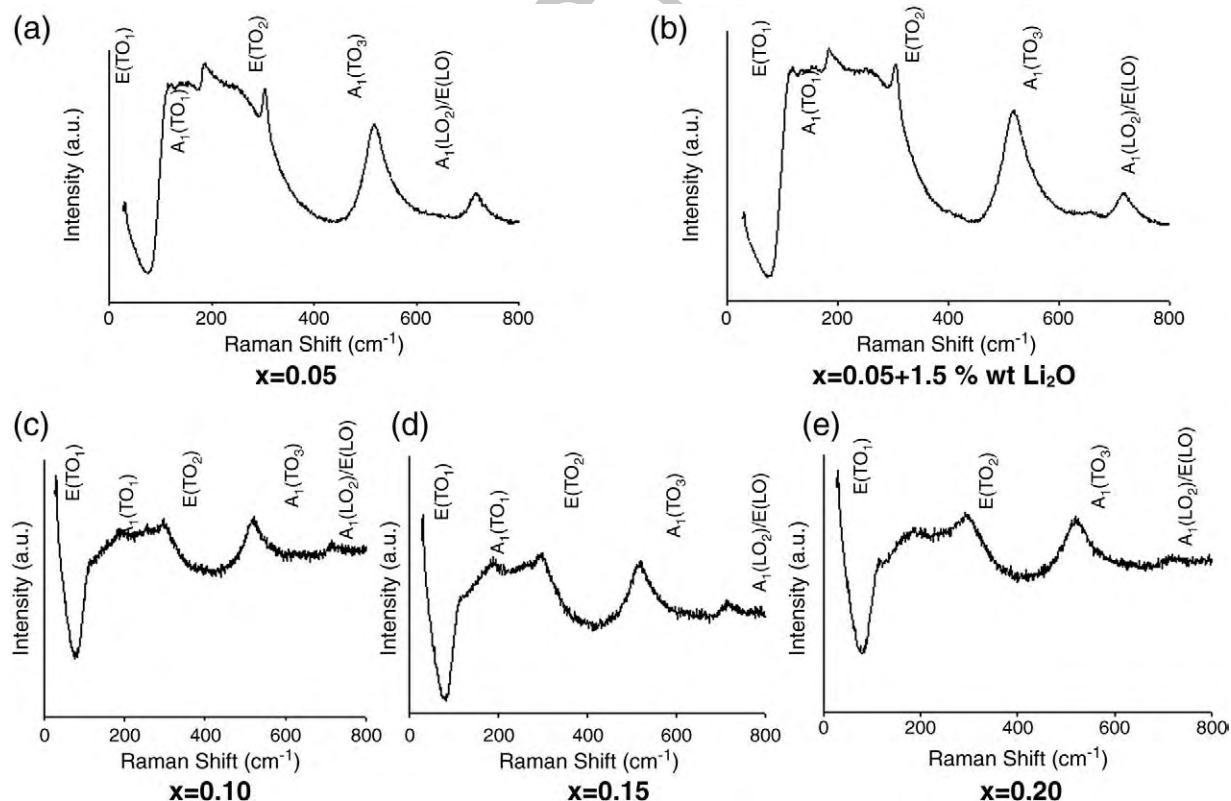


Fig. 2. The Raman spectra of (a, c–e) $\text{Ba}(\text{Zr}_x\text{Ti}_{1-x})\text{O}_3$ powders calcined at 1100 °C, 2 h and (b) $\text{Ba}(\text{Zr}_{0.05}\text{Ti}_{0.95})\text{O}_3$ powders with 1.5 wt.% Li_2O calcined at 700 °C, 10 h.

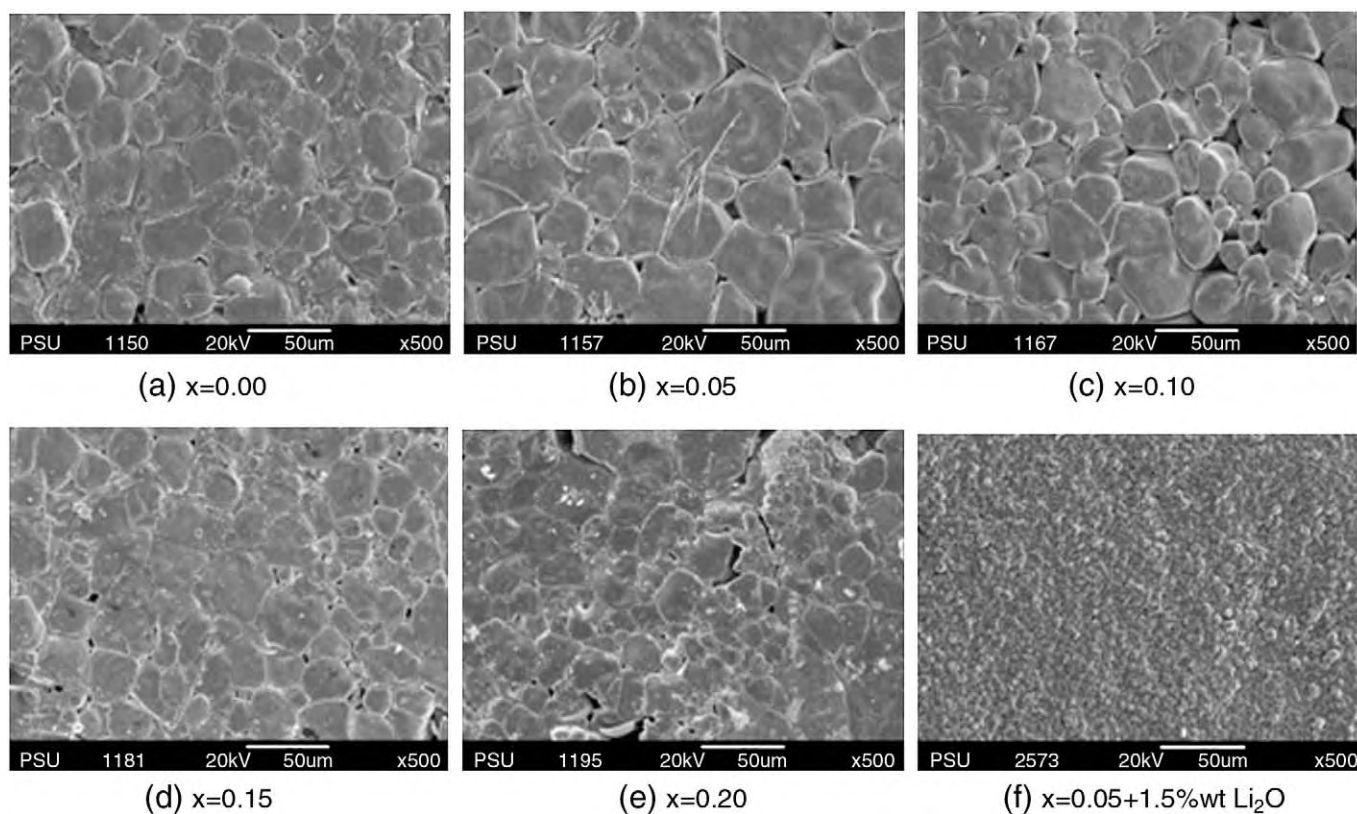


Fig. 3. SEM images for $\text{Ba}(\text{Zr}_x\text{Ti}_{1-x})\text{O}_3$ ceramics.

size in Li-doped sample and this leads to a wider dielectric curve with a lower dielectric constant which, however, remains relatively high when compared to conventional ceramics. This material is, thus, promising for use in various applications.

Table 1

Mean particle size, d of the BZT powders and density and average grain size of the BZT ceramics.

$\text{Ba}(\text{Zr}_x\text{Ti}_{1-x})\text{O}_3$ powders	S_w (m ² /g)	d (μm)	Density (g/cm ³)	Average grain size (μm)
$x = 0.00$	2.14	0.46	5.04	39.60
$x = 0.05$	3.45	0.28	5.06	27.54
$x = 0.05 + 1.5\text{wt.}\% \text{Li}_2\text{O}$	1.66	0.13	5.59	4.00
$x = 0.10$	3.19	0.29	5.09	21.63
$x = 0.15$	3.49	0.28	5.38	20.19
$x = 0.20$	3.92	0.25	5.41	15.94

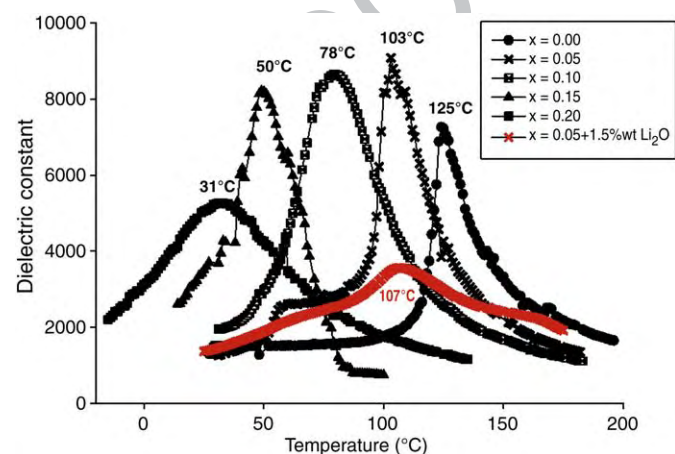


Fig. 4. Temperature dependence of the dielectric constant for BZT samples.

The electromechanical properties for all the samples were summarized in Table 2. The dielectric constant of the low-sintering-temperature $\text{Ba}(\text{Zr}_{0.05}\text{Ti}_{0.95})\text{O}_3$ was slightly decreased. The dielectric loss was also lower. The sample at this composition exhibits the relatively high piezoelectric response and good electromechanical coupling. It is known that the higher the number of polarizable directions aligned to a poling field, the larger the piezoelectric coefficient is. Possible polar directions in the tetragonal, orthorhombic, and rhombohedral structures are six, twelve, and eight, respectively. This corresponded to the crystalline phases identified earlier that the $\text{Ba}(\text{Zr}_{0.05}\text{Ti}_{0.95})\text{O}_3$ is orthorhombic while the $\text{Ba}(\text{Zr}_{0.10}\text{Ti}_{0.90})\text{O}_3$ and $\text{Ba}(\text{Zr}_{0.15}\text{Ti}_{0.85})\text{O}_3$ are rhombohedral.

4. Conclusions

Barium zirconate titanate of different Zr contents was studied their physical and electromechanical properties and the use of lithium oxide as sintering aid was evaluated. With the additive, the densification of the BZT took place at 900 °C which is lower than the melting points of the conventional conductive materials like silver and gold. The effect of sintering aid on the physical properties was

Table 2

Room-temperature electromechanical properties of the BZT ceramics.

$\text{Ba}(\text{Zr}_x\text{Ti}_{1-x})\text{O}_3$	d_{33} coefficient (pC/N ⁻¹)	d_{31} coefficient (pC/N ⁻¹)	k_p (%)	Dielectric constant (1 kHz)	Dielectric loss (1 kHz)
$x = 0.00$	101 ± 5.0	-25.65	46	1302	0.037
$x = 0.05$	126 ± 5.0	-23.95	44	1361	0.041
$x = 0.05 + 1.5\text{wt.}\% \text{Li}_2\text{O}$	120 ± 5.0	-22.25	44	1250	0.026
$x = 0.10$	83 ± 5.0	-24.56	44	1957	0.045
$x = 0.15$	36 ± 5.0	-19.27	44	3704	0.060
$x = 0.20$	-	-	-	5118	0.070

152 observed in the low-sintering-temperature BZT, however, their good
153 electromechanical properties remained. Mechanically activated pow-
154 ders of this material are attractive for, e.g., making paste materials
155 used in conventional screen-printing techniques [4].

156 Acknowledgements

157 The authors thank the Office of the Higher Education Commission,
158 Thailand for the grant support under the program Strategic Scholar-
159 ships for Frontier Research Network for the Joint Ph.D. Program of Thai
160 Doctoral Degree and the National Nanotechnology Center (NANOTEC),
161 NSTDA, Ministry of Science and Technology, through its program of
162 Center of Excellence Network at PSU.
178

References

- | | |
|--|-----|
| [1] Shrout RT, Zhang SJ. <i>J Electroceram</i> 2007;19:111. | 164 |
| [2] Yu Z, Ang C, Gua R, Bhalla AS. <i>J Appl Phys</i> 2002;92:1489. | 165 |
| [3] Yu Z, Ang C, Gua R, Bhalla AS. <i>Mater Lett</i> 2007;61:326. | 166 |
| [4] Ginet P, Lucat C, M enil F. <i>Int J Appl Technol</i> 2007;4(5):423. | 167 |
| [5] Stojanovic BD, Foschini CR, Pavlovic VB, Pavlovic VM, Pejovic V, Varela JAV. <i>Ceram Int</i> 2002;28:293. | 168 |
| [6] Tick T, Per anti J, Jantunen H, Usim aki AU. <i>J Eur Ceram Soc</i> 2008;28:837. | 169 |
| [7] Jiwei Z, Yao X, Zhang L, Shen B, Haydn C. <i>J Cryst Growth</i> 2004;262:341. | 170 |
| [8] Jeong SJ, Lee DS, Park EC, Song JS. <i>J Electrocerm</i> 2006;17:537. | 171 |
| [9] Berlincourt Piezo d_{33} meter manual. (1974). | 172 |
| [10] Mason WP, Jaffe H. <i>Proc IRE</i> 1954;42:921. | 173 |
| [11] Moura F, Sim oes AZ, Stojanovic BD, Zaghete MA, Longo E, Varela JA. <i>J Alloy and Compound</i> 2008;462:129. | 174 |
| [12] Dobal PS, Dixit A, Katiyar RS, Yu Z, Gua R, Bhalla RS. <i>J Appl Phys</i> 2001;89:8085. | 175 |
| | 176 |
| | 177 |

UNCORRECTED PROOF